

Moiré Intralayer Excitons in a $\text{MoSe}_2/\text{MoS}_2$ Heterostructure

Nan Zhang,^{†,¶} Alessandro Surrente,^{†,¶} Michał Baranowski,^{†,§} Duncan K. Maude,[†] Patricia Gant,[‡] Andres Castellanos-Gomez,[‡] and Paulina Plochocka^{*,†}

[†]*Laboratoire National des Champs Magnétiques Intenses, UPR 3228,
CNRS-UGA-UPS-INSA, Grenoble and Toulouse, France*

[‡]*Materials Science Factory, Instituto de Ciencia de Materiales de Madrid (ICMM),
Consejo Superior de Investigaciones Científicas (CSIC), Sor Juana Ins de la Cruz 3, 28049
Madrid, Spain*

[¶]*These authors contributed equally to the work*

[§]*Department of Experimental Physics, Faculty of Fundamental Problems of Technology,
Wroclaw University of Science and Technology, 50-370 Wroclaw, Poland*

E-mail: paulina.plochocka@lncmi.cnrs.fr

Abstract

Spatially periodic structures with a long range period, referred to as moiré pattern, can be obtained in van der Waals bilayers in the presence of a small stacking angle or of lattice mismatch between the monolayers. Theoretical predictions suggest that the resulting spatially periodic variation of the band structure modifies the optical properties of both intra and interlayer excitons of transition metal dichalcogenides heterostructures. Here, we report on the impact of the moiré pattern formed in a $\text{MoSe}_2/\text{MoS}_2$ heterobilayer encapsulated in hexagonal boron nitride. The periodic in-plane potential results in a splitting of the MoSe_2 exciton and trion in both emission

and absorption spectra. The observed energy difference between the split peaks is fully consistent with theoretical predictions.

Keywords

Transition metal dichalcogenides, van der Waals heterostructures, moiré pattern, moiré excitons, valley polarization

The vertical stacking of atomically thin planes of layered solids provides a rich playground to expand the properties of the constituting layers, which gives rise to new and attractive features.^{1,2} The possibility to combine a plethora of different layered materials allows to efficiently tailor the properties of van der Waals heterostructures. In particular, this approach has been successfully employed for transition metal dichalcogenides (TMDs).^{3,4} Sandwiching TMD monolayers between hexagonal boron nitride (hBN) improves significantly their optical and electrical properties,^{5,6} paving the way to access their rich excitonic and transport physics.⁵⁻¹⁴ Bringing TMD monolayers in close contact with graphene makes it possible to tune controllably the band gap of the TMD, owing to the locally different dielectric environment.¹⁵ Stacking different semiconducting TMDs also allows to overcome the limitations of isolated TMD monolayers in valleytronic applications,¹⁶⁻²⁰ such as very short exciton and valley polarization lifetimes.²¹⁻²⁵ TMD heterostructures exhibit type II band alignment,^{3,4,26} which leads to the formation of interlayer excitons with radiative and valley lifetimes up to five orders of magnitude longer than for intralayer excitons.²⁷⁻³² The helicity of the long lived interlayer exciton emission can be further controlled by the polarization of the excitation laser,^{28,31-34} which makes van der Waals heterostructures attractive for valleytronic applications.

Due to the weak van der Waals interactions in heterostructures, the lattice constant of each monolayer does not conform to that of the underlying substrate. If monolayers with different lattice parameters or with a non-zero (but small) stacking angle are overlaid, a

moiré pattern is formed.^{35–40} The resulting in-plane superlattice potential has a tremendous impact on the electronic properties of the van der Waals heterostructures, opening up new directions for material engineering, which relies on the relative orientation of the constituting layers. The physics related to the moiré pattern has been studied in hBN/graphene heterostructures, where the induced periodic potential leads to the formation of new Dirac cones, opening of a band gap, and the appearance of Hofstadter butterfly states.^{37,38,41–43} The moiré pattern formed in TMD heterostructures is also expected to have a large influence on their properties.^{39,40,44,45} According to theoretical predications, the moiré pattern should result in a periodically modulated potential with minima for both intra^{39,45} and interlayer^{39,44} excitons, thus forming an array of quantum dots. Moreover, spatially varying selection rules for interlayer excitons can result in an emission with helicity opposite with respect to that of the excitation laser.^{39,44} Finally, the variation of the confinement potential for different atomic registries should lead to an energy splitting of both the intra⁴⁵ and interlayer transitions.^{39,44} The formation of a moiré pattern and the related periodic potential fluctuations have been confirmed recently using scanning tunneling microscopy.^{40,46} However, direct experimental evidence of the influence of the moiré pattern on the optical properties of TMD heterostructures has remained elusive so far. The only indirect indication is related to the observation of counter polarized emission of the interlayer exciton.^{31–33,47}

In this work, we show how the observed splitting of the intralayer exciton and trion in a monolayer MoSe₂ assembled in a heterostructure with MoS₂ and encapsulated in hBN is a direct consequence of the moiré pattern formed between MoSe₂ and MoS₂. The high quality of our heterostructure (typical full width at half maximum of the exciton and trion photoluminescence, PL, peaks ~ 5 meV) allows us to reveal the splitting of the trion and exciton lines both in PL and reflectivity spectra. The structure of the intralayer exciton transitions can be observed consistently over the whole area where the two materials overlap, while we observed no splitting out of the heterostructure area. The energy splitting of the peaks and their temperature dependence are in agreement with the expected influence of

the moiré potential on the intralayer exciton species. Our results provide a clear optical fingerprint of the effect of the moiré potential on intralayer excitons of a monolayer TMD.

We show a micrograph of the fabricated heterostructure in Fig. 1(a). It consists of a monolayer MoSe₂ flake, indicated by a blue dashed line, partially covered by a MoS₂ monolayer (white dashed line). The nominal angle between the MoS₂ and MoSe₂ crystal axis is $\sim 0^\circ$. Second harmonic spectroscopy confirmed that the actual stacking angle is $\sim 1^\circ$, as discussed in the Supporting Information. Both layers are fully encapsulated in hBN and this van der Waals stack is deposited on a SiO₂ substrate. A more detailed description of the fabrication procedure is provided in Methods. Additional microscope images of the flakes used to prepare the heterostructure are shown in the Supporting Information. A representative, broad range PL spectrum of our heterostructure at $T = 5$ K is presented in Fig. 1(b). The peaks at 1.615 eV and 1.644 eV arise from the radiative recombination of the intralayer trion and exciton of MoSe₂, respectively. The weaker PL peaks centered at 1.94 eV and 1.87 eV are assigned to the recombination of neutral excitons and to excitonic complexes bound to defects in MoS₂,^{5,48} respectively. The low energy peak at 1.37 eV stems from the interlayer exciton emission, formed due to the spatial separation of charge carriers in a type II heterostructure, as schematically shown in the inset of Fig. 1(b).^{31,32} In this work, we focus on the properties of intralayer excitons. PL intensity maps of intralayer MoS₂ and MoSe₂ are presented in Fig. 1(c,d), respectively. The MoSe₂ PL intensity of Fig. 1(d) is suppressed in the heterostructure area, due to the interlayer charge transfer.^{49,50} The strongly modified optical properties in the heterostructure area are an indication of a good coupling between the layers, characteristic for 0° stacking angle.⁵¹

On a fully hBN-encapsulated MoSe₂ monolayer, the PL spectrum consists of two peaks, attributed to charged and neutral exciton (see Fig. 2(a)). In contrast, the MoSe₂ exciton and trion PL from the heterostructure region reveals a double peak structure, as shown in Fig. 2(b). We label these features X_L (T_L) and X_H (T_H), to refer to higher and lower energy transition of the exciton (trion). A similar double structure is also observed for the MoS₂

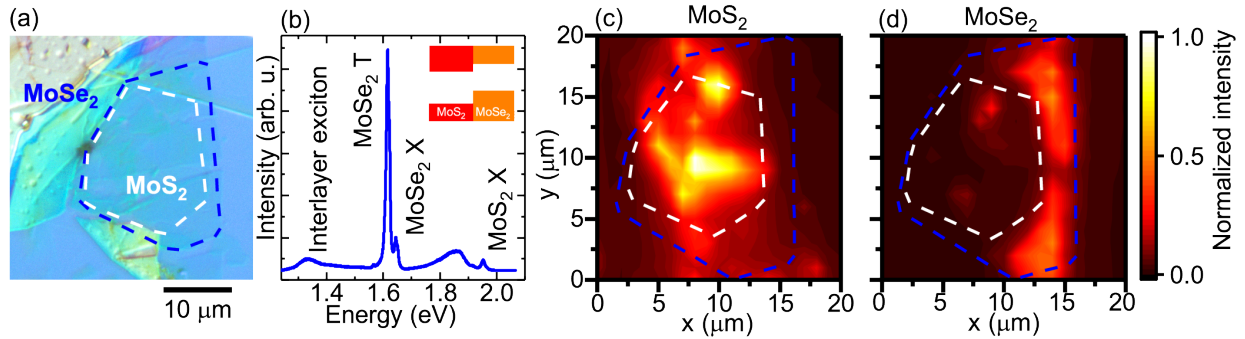


Figure 1: (a) Optical microscope image of the MoS₂/MoSe₂ heterostructure encapsulated in hBN. The blue and white dashed lines indicate the contours of the MoSe₂ and MoS₂ flakes. (b) Broad range PL spectrum of the heterostructure. Inset: schematic band alignment of a MoSe₂/MoS₂ heterostructure. Normalized PL intensity maps of (c) MoS₂ and (d) MoSe₂.

free exciton emission (see Supporting Information). Importantly, the splitting of the exciton is also visible in the reflectivity spectrum of Fig. 2(b), unequivocally demonstrating that it is related to a free exciton transition rather than to the emission from excitons bound to defects. The presence of a double PL peak in the heterostructure region is consistent with the expected effect of the moiré pattern on the intralayer excitonic complexes. According to theoretical predictions, the stacking of two lattice mismatched TMD monolayers induces a spatially periodic fluctuation of the potential, felt by the excitons,^{39,40,44,45} with local minima related to different atomic registries.³⁹ The period of the moiré pattern is in the range of a few to tens of nanometers (see Supporting Information for a discussion specific to our heterostructure). Therefore, the spatial resolution of our far field optical measurements is not sufficient to resolve the spatial variation of the emission energy of excitons located at different potential minima. Nevertheless, the emission from different optically active minima of the moiré pattern can be spectrally resolved in our high quality sample. The double structure of the exciton and trion peaks is consistently observed only in the heterostructure, while it is completely absent in monolayer regions. This is summarized in Fig. 2(c), where the spatial map highlights the areas where the splitting is observed. To verify that the observed splitting is a direct consequence of the moiré pattern, we prepared two control samples (presented in Supporting Information), which consist of MoS₂/MoSe₂ heterostructures with stacking

angles of $\sim 20^\circ$ and $\sim 60^\circ$. In former sample, the period of the moiré pattern is significantly smaller than the spatial extension of the intralayer exciton wave function and, as expected, we did not observe any splitting in the PL spectrum of the MoSe₂ exciton or trion. In latter sample, we systematically observe the splitting of the exciton and trion PL peaks of MoSe₂, whenever the excitation is performed within the heterostructure area. This is consistent with theoretical predictions,³⁹ and with the long range spatial period of the moiré pattern formed in the case of $\sim 0^\circ$ and $\sim 60^\circ$ stacking angle (see Supporting Information).

In Fig. 2(d), we show the spatial variation of the exciton and trion PL energy along the dashed line crossing the heterostructure in Fig. 2(c). The slice starts and ends at positions on the sample where PL is observed. A direct comparison of the spectrum measured in the heterostructure region with one measured outside (see Fig. 2(a,b)) reveals that the double structure results from the appearance of a new energy peak on the high energy side of the main exciton and trion emission. The energies of the emission lines observed in isolated monolayers are nearly identical to the X_L and T_L lines observed in the heterostructure, as highlighted by the vertical lines in Fig. 2(a,b). This is in agreement with the prediction that the exciton states related to the moiré pattern should appear as peaks on the high energy side of the main PL peaks.^{39,45} This observation, along with the fact that the double peak structure appears over a vast area in the heterostructure and not only at its edges,¹⁵ allows us to rule out the variation of the dielectric screening related to the presence of the MoS₂ monolayer as the origin of the observed doublet structure. Since the dielectric constant of MoS₂ is higher than that of hBN,⁵² a dielectric screening effect would lead to the appearance of lower energy peaks when the excitation is performed on the heterostructure.¹⁵ We also exclude a strain-related origin of the new peak by noting that the red shift of the A_{1g} mode of MoSe₂ in the heterostructure would suggest tensile strain of MoSe₂ comprised in the heterostructure, which is not compatible with the appearance of a high energy peak in the PL spectrum^{53–55} (see Supporting Information for more details). Finally, the observed energy scale of the PL peaks splitting (~ 6 – 12 meV) is in agreement with the energy scale

of potential variations predicted for the related $\text{MoS}_2/\text{WSe}_2$ heterostructure.³⁹

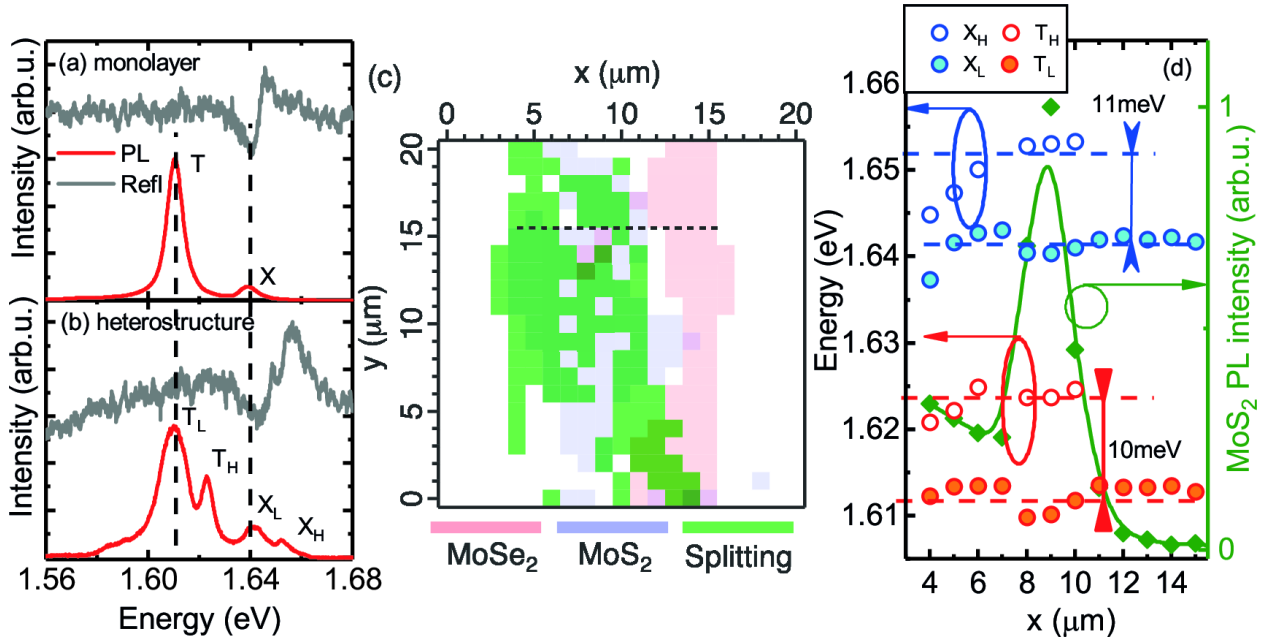


Figure 2: PL and reflectivity spectra of MoSe_2 measured in (a) monolayer and (b) heterostructure. (c) Spatial map showing the presence of MoSe_2 transition splitting, overlaid with the areas of most intense PL of MoS_2 and MoSe_2 . (d) Energy of the observed MoSe_2 transitions (blue and red dots) extracted along the horizontal dashed line of panel (c). Open circles correspond to high energy peaks observed only in the heterostructure, closed circles represent low energy transitions observed in all the MoSe_2 flake. Green diamonds: MoS_2 PL intensity.

In Fig. 3, we summarize the temperature dependence of the MoSe_2 PL measured on the heterostructure. As for all Mo-based TMDs, we observe a decrease of the PL intensity with increasing temperature.⁵⁶ We notice in particular a faster decrease of the intensity of the trion PL, which can be no longer resolved at temperatures larger than ~ 100 K,⁴⁸ consistent with the smaller binding energy of this complex as compared to the exciton. Concerning the states split by the moiré potential, the intensity of the high energy peaks X_H and T_H decreases more rapidly than that of the low energy peaks. For temperatures higher than ~ 90 K, corresponding to a thermal energy of ~ 7.7 meV, the X_H and T_H features are no longer resolved. This is illustrated in the inset of Fig. 3, where we plot the ratio of the intensities of the high energy peaks I_H normalized by the intensities of the corresponding low energy peaks I_L . The faster quenching of the X_H and T_H emission further supports

the moiré pattern as the origin of the trion and exciton doublet. A smaller confinement is expected for the higher energy states,³⁹ hence with increasing thermal energy these excitons can be detrapped more easily via thermally activated phonon scattering out of the minima of the moiré potential. From the temperature dependence of the intensity of X_H , an activation energy of ~ 26 meV can be extracted (see Supporting Information). This value compares to the depth of the moiré potential for intralayer excitons of 12–19 meV, depending on the stacking of the heterobilayer.³⁹ This behaviour is fully consistent with the observation of a more rapid thermal quenching of the PL of high energy moiré states observed in the interlayer exciton.⁵⁷

We investigated the valley polarization properties of the intralayer MoSe₂ excitons by exciting the PL with circularly polarized light and detecting the co-polarized and cross-polarized circular polarization PL components. We show the PL spectra of the isolated monolayer and of the monolayer comprised in a heterostructure in Fig. 4(a,b). The degree of circular polarization P_c of the PL, $P_c = (I_{co} - I_{cross}) / (I_{co} + I_{cross})$, is always positive (see green bars in Fig. 4). The degree of circular polarization is very similar for the heterostructure and monolayer regions and amounts to about 10% and 13% for the trion and the exciton, respectively. There is no significant difference between the polarization of high and low energy transitions in heterostructure. This suggests that, consistent with theoretical predictions,³⁹ the selection rules for the intralayer exciton transitions are not influenced by the presence of the moiré pattern, thus all transitions have the same polarization. This can be explained by considering that the rotational symmetry of the transitions does not change in the plane of the monolayers, in contrast to the interlayer transition for which the helicity of the emitted light varies across the moiré pattern.^{39,44} The observed significant polarization is surprising considering that we excite far from excitonic transitions of MoSe₂.^{48,58–60} This effect might be related to the encapsulation in hBN because we observe a similar degree of circular polarization in both the heterostructure and monolayer regions, although the exact reason the relatively high degree of polarization after encapsulation requires additional investigation.

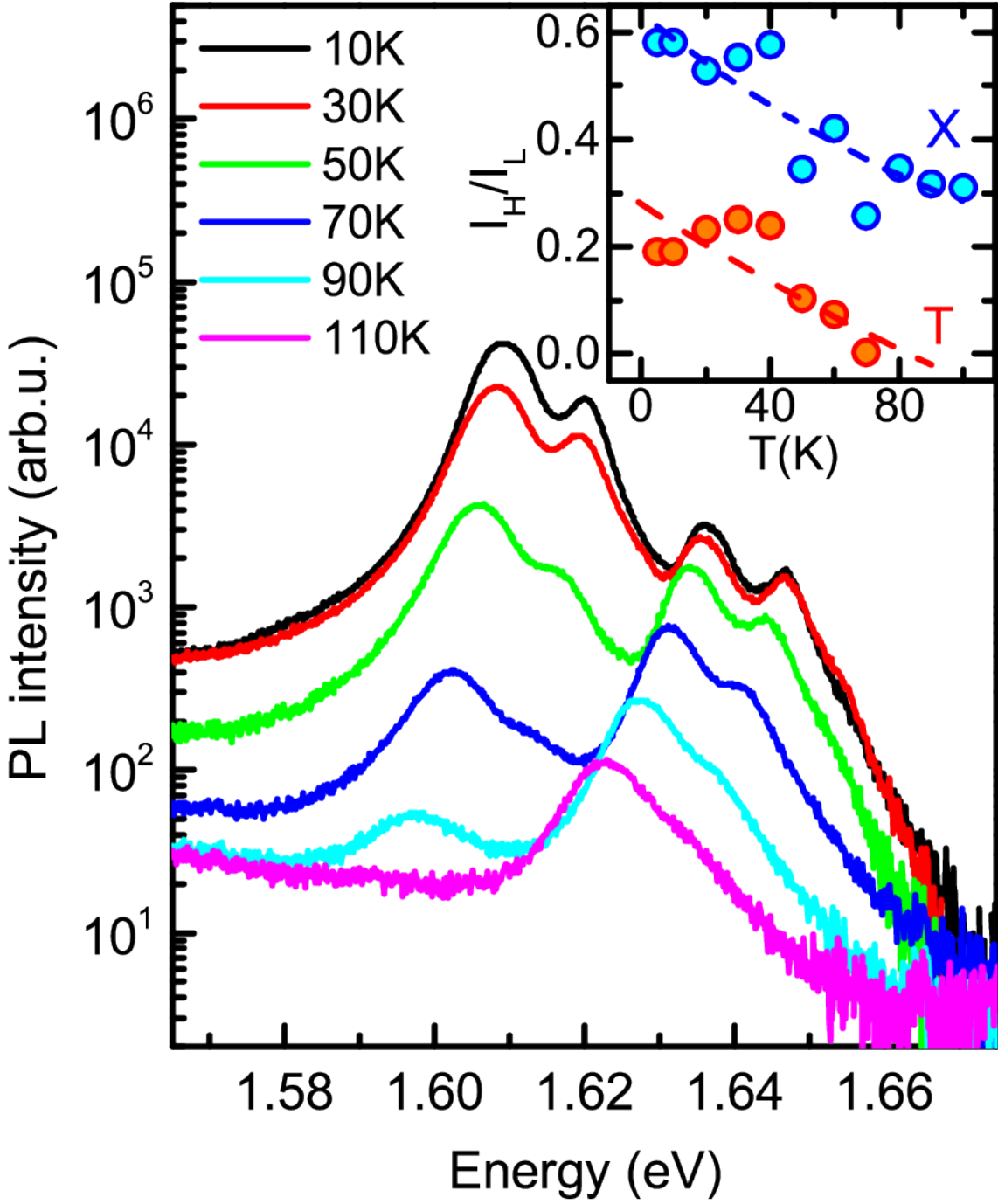


Figure 3: Temperature dependence of MoSe₂ PL. Inset: ratio of intensities of the high to low energy exciton and trion I_H/I_L .

Finally, we investigate the dynamics of the trion and exciton in MoSe₂. The spectrally resolved temporal evolution of the PL measured in the heterostructure area is shown in Fig. 4(c). Similar data acquired on an isolated MoSe₂ monolayer is shown in the Supporting Information. In the streak image of Fig. 4(c), the four PL peaks are well resolved, with the dynamics of the excitonic transition being significantly faster than those of the trions. To obtain more quantitative information, we extract the decay curves corresponding to MoSe₂ trion and exciton transitions in monolayer and heterostructure regions in Fig. 4(d,e), respectively. PL decays of all trion and exciton species can be fitted well using a single exponential, convoluted with a Gaussian curve to account for the instrument response function of the system. From this fitting, we extract the PL life times. There are no significant differences between PL decay times in the monolayer and heterostructure areas or between X_H (T_H) and X_L (T_L) transitions. For the exciton transitions, the PL decay time is ~ 14 ps, while for the trion it is ~ 70 ps. We notice, however, that the PL decay time of the exciton is close to the resolution of our system, therefore the dynamics of the two exciton states might be slightly different. The faster decay of the high energy trion is consistent with the observation on the dynamics of high energy interlayer exciton states in a moiré potential, where this behaviour has been attributed to the possible relaxation of high energy states to the low energy states.⁵⁷

The overall similar decay times of the high and low energy transitions suggest that the moiré potential does not affect significantly the oscillator strength of the transitions. This can be understood as a result of the slow spatial variation of moiré potential (a few to tens of nm, depending on the stacking angle and the lattice mismatch of the heterobilayer) compared to the exciton size in TMD monolayers (~ 1 nm).^{9,61} Therefore, the wave function of intralayer excitons is not significantly affected by the confinement induced by the moiré pattern. Interestingly, despite a clear drop of the PL intensity in the heterostructure area (Fig. 1), the decay times of the trion and exciton PL are very similar to those observed in monolayer regions. This indicates that the charge transfer between the layers occurs im-

mediately after excitation and is effective only for hot carriers, in agreement with previous pump probe measurements.⁴⁹ The observed PL is related to thermalized excitons and the unchanged decay times show that they are not affected by the interlayer transfer. This might be the result of the weak localization potential induced by the moiré pattern. A larger intensity of the interlayer exciton PL has been observed in MoSe₂/MoS₂ heterostructures³¹ with increasing temperature. This is probably the hallmark of the thermal activation of excitons from shallow traps, represented by the moiré potential, followed by interlayer transfer. However, further studies are needed to clarify this aspect, notably to distinguish it from a possible indirect character in k-space of the interlayer transitions.^{30,62}

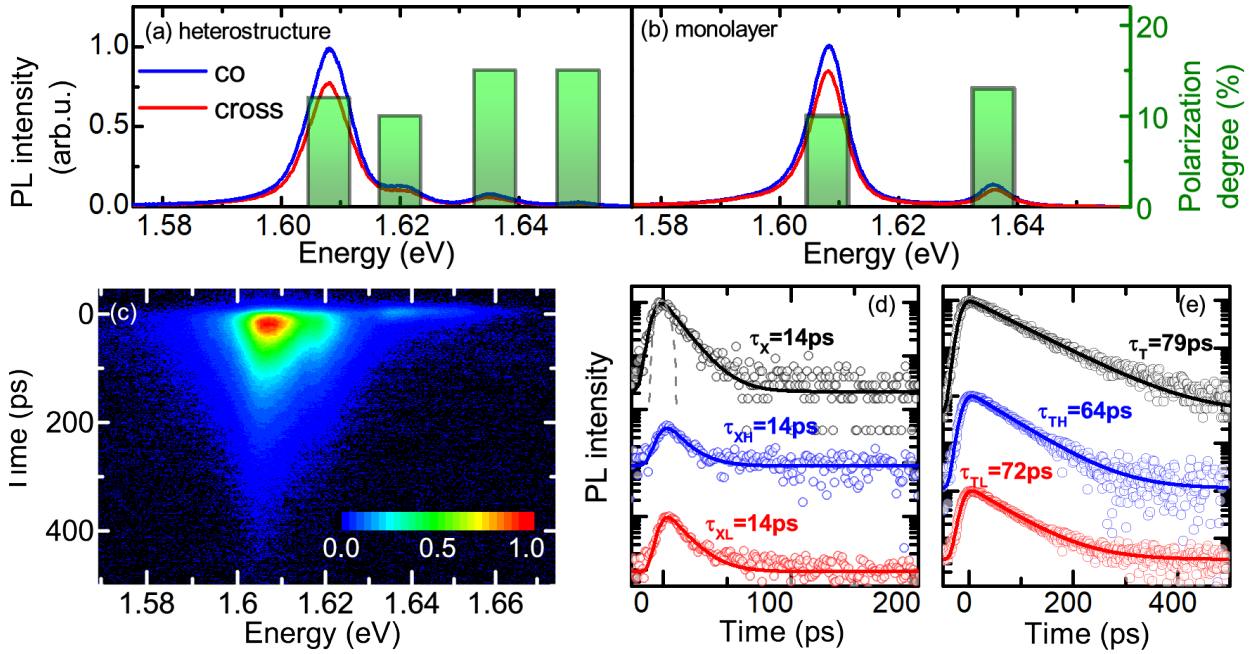


Figure 4: Circularly polarization resolved PL spectrum of MoSe₂ measured (a) in and (b) out of the heterostructure. The green bars represent the degree of circular polarization of the peaks. (c) Spectrally resolved PL time evolution measured in the heterostructure area. (d) Decay curves (open circles) corresponding to low (red) and high (blue) energy of MoSe₂ exciton and (e) trion from the heterostructure and decay of exciton PL outside heterostructure (black) together with fitted monoexponential decays. The extracted decay time constants are specified above the corresponding curves. The instrument response function is traced in dashed line in panel (d).

In conclusion, we have demonstrated the impact of the moiré pattern formed in a MoS₂/MoSe₂ heterostructure on the optical spectra of the intralayer exciton species. The

potential fluctuations resulting from locally different atomic registries split the trion and exciton transitions of MoSe₂ and MoS₂ into two peaks related to optically active local minima of the moiré potential. The nature of these doublets has been confirmed by detailed spatial mapping of the PL and by the temperature dependence of their PL. Polarization resolved measurements reveal that the selection rules of the transitions do not change with respect to the case of isolated monolayers. The PL dynamics show that moiré induced potential does not change significantly the oscillator strength of the transitions. However, the moiré potential may be responsible for the suppression of the interlayer transfer of thermalized excitons. All of the results presented are in agreement with the theoretically predicted influence of moiré pattern on intralayer excitons in transition metal dichalcogenides.

Methods

Sample preparation. The samples have been prepared by all-dry deterministic transfer of mechanically exfoliated flakes.^{63,64} hBN flakes have been exfoliated from commercially available hBN powder (Momentive, Polarthem grade PT110) using Nitto tape (Nitto Denko corp. SPV 224). MoS₂ and MoSe₂ flakes have been also exfoliated with Nitto tape from naturally occurring molybdenite mineral (Molly Hill mine, Quebec, Canada) and synthetic bulk MoSe₂ grown by chemical vapour transport. The flakes cleaved from the bulk source of material are transferred onto a Gelfilm (WF x4 6.0 mil by Gelpak) that is used as a viscoelastic stamp to perform the deterministic transfer. MoS₂ and MoSe₂ monolayers are selected from their transmittance and reflection spectra prior to their transfer.⁶⁵ Monolayers with large faceted edges were used for the assembly of the heterostructures. The straight edges of the MoS₂ and MoSe₂ were aligned with accuracy better than 0.5° during the transfer.

Optical spectroscopy. For optical measurements, the sample was mounted on the cold finger of a helium flow cryostat with a quartz optical window. Unless stated otherwise, all measurements have been performed at $T = 5$ K. Time resolved PL measurements were

performed using a CW frequency doubled solid state laser emitting at 532 nm. The circularly polarization resolved PL was excited with the frequency-doubled output of an optical parametric oscillator (OPO), synchronously pumped by a mode-locked Ti:sapphire laser and tuned to 600 nm. The temporal pulse width is typically 300 fs, with a repetition rate of 80 MHz. The instrument response function of the system, shown in Fig. 4(d), has a half width at half maximum of 6 ps. The excitation laser beam was focused on the sample using a 50 \times microscope objective with a numerical aperture of 0.55, giving a spot size of approximately 1 μ m diameter. The excitation power used for time-integrated measurements was 20 μ W. The emitted PL was collected through the same objective and directed to a spectrometer equipped with a liquid nitrogen cooled charge-coupled device (CCD) camera. For time-resolved measurements, the excitation was provided by the OPO tuned to 530 nm, using an average power of 100 μ W. The collected signal was spectrally dispersed using a monochromator and detected using a streak camera. Second harmonic measurements were performed in a similar setup. The Ti:sapphire laser was used as the excitation source. The laser light was polarized via a broadband polarizer and a halfwave plate was used to control the direction of the linear polarization of the fundamental wave. The laser was focused onto the sample using the same 50 \times microscope objective used for PL measurements. The same set of halfwave plate and linear polarizer were used to analyze the polarization of the second harmonic signal, thus insuring that only the component of the second harmonic parallel to the polarization of the excitation was detected. The second harmonic signal was separated by the fundamental component by making use of a shortpass filter. The signal was finally detected by the spectrometer combined with the CCD.

Supporting Information Available

The following files are available free of charge. Micrograph of different stages of preparation of the van der Waals stack, second harmonic spectroscopy of the heterostructure presented in

the main text, period of moiré pattern as a function of the stacking angle, microPL spectra of additional devices with $\sim 20^\circ$ and $\sim 60^\circ$ stacking angle, activation energy of high energy exciton peak, Raman spectra of isolated MoSe₂ and MoSe₂ in a heterostructure, maps of the energy splitting of MoSe₂ exciton and trion, low temperature μ PL spectrum of MoS₂ with split exciton peak, and time resolved PL of isolated MoSe₂.

Acknowledgement

This work was partially supported by BLAPHENE and STRABOT projects, which received funding from the IDEX Toulouse, Emergence program, “Programme des Investissements d’Avenir” under the program ANR-11-IDEX-0002-02, reference ANR-10-LABX-0037-NEXT. N.Z. holds a fellowship from the China Scholarship Council (CSC). M.B. appreciates support from the Polish Ministry of Science and Higher Education within the Mobilnosc Plus program (grant no. 1648/MOB/V/2017/0). This project has also received funding from the European Research Council (ERC) under the European Union’s Horizon 2020 research and innovation programme (grant agreement no. 755655, ERC-StG 2017 project 2D-TOPSENSE) and from the EU Graphene Flagship funding (Grant Graphene Core 2, 785219).

References

- (1) Geim, A. K.; Grigorieva, I. V. Van der Waals heterostructures. *Nature* **2013**, *499*, 419–425.
- (2) Novoselov, K.; Mishchenko, A.; Carvalho, A.; Neto, A. C. 2D materials and van der Waals heterostructures. *Science* **2016**, *353*, aac9439.
- (3) Dong, R.; Kuljanishvili, I. Progress in fabrication of transition metal dichalcogenides heterostructure systems. *Journal of Vacuum Science & Technology B, Nanotechnology*

- and Microelectronics: Materials, Processing, Measurement, and Phenomena* **2017**, *35*, 030803.
- (4) Zhou, X.; Hu, X.; Yu, J.; Liu, S.; Shu, Z.; Zhang, Q.; Li, H.; Ma, Y.; Xu, H.; Zhai, T. 2D Layered Material-Based van der Waals Heterostructures for Optoelectronics. *Advanced Functional Materials* **2018**, *28*, 1706587.
- (5) Cadiz, F.; Courtade, E.; Robert, C.; Wang, G.; Shen, Y.; Cai, H.; Taniguchi, T.; Watanabe, K.; Carrere, H.; Lagarde, D.; Manca, M.; Amand, T.; Renucci, P.; Tongay, S.; Marie, X.; Urbaszek, B. Excitonic linewidth approaching the homogeneous limit in MoS₂-based van der Waals heterostructures. *Physical Review X* **2017**, *7*, 021026.
- (6) Fallahazad, B.; Movva, H. C.; Kim, K.; Larentis, S.; Taniguchi, T.; Watanabe, K.; Banerjee, S. K.; Tutuc, E. Shubnikov–de Haas oscillations of high-mobility holes in monolayer and bilayer WSe₂: Landau level degeneracy, effective mass, and negative compressibility. *Physical Review Letters* **2016**, *116*, 086601.
- (7) Robert, C.; Semina, M.; Cadiz, F.; Manca, M.; Courtade, E.; Taniguchi, T.; Watanabe, K.; Cai, H.; Tongay, S.; Lassagne, B.; Renucci, P.; Amand, T.; Marie, X.; Glazov, M. M.; Urbaszek, B. Optical spectroscopy of excited exciton states in MoS₂ monolayers in van der Waals heterostructures. *Physical Review Materials* **2018**, *2*, 011001.
- (8) Manca, M.; Glazov, M.; Robert, C.; Cadiz, F.; Taniguchi, T.; Watanabe, K.; Courtade, E.; Amand, T.; Renucci, P.; Marie, X.; Wang, G.; Urbaszek, B. Enabling valley selective exciton scattering in monolayer WSe₂ through upconversion. *Nature Communications* **2017**, *8*, 14927.
- (9) Stier, A. V.; Wilson, N. P.; Velizhanin, K. A.; Kono, J.; Xu, X.; Crooker, S. A. Magneto-optics of Exciton Rydberg States in a Monolayer Semiconductor. *Physical Review Letters* **2018**, *120*, 057405.

- (10) Chen, S.-Y.; Goldstein, T.; Tong, J.; Taniguchi, T.; Watanabe, K.; Yan, J. Superior Valley Polarization and Coherence of 2s Excitons in Monolayer WSe₂. *Physical Review Letters* **2018**, *120*, 046402.
- (11) Xu, S.; Shen, J.; Long, G.; Wu, Z.; Bao, Z.-q.; Liu, C.-C.; Xiao, X.; Han, T.; Lin, J.; Wu, Y.; Lu, H.; Hou, J.; An, L.; Wang, Y.; Cai, Y.; Ho, K. M.; He, Y.; Lortz, R.; Zhang, F.; Wang, N. Odd-Integer Quantum Hall States and Giant Spin Susceptibility in p-Type Few-Layer WSe₂. *Physical Review Letters* **2017**, *118*, 067702.
- (12) Movva, H. C.; Fallahazad, B.; Kim, K.; Larentis, S.; Taniguchi, T.; Watanabe, K.; Banerjee, S. K.; Tutuc, E. Density-Dependent Quantum Hall States and Zeeman Splitting in Monolayer and Bilayer WSe₂. *Physical Review Letters* **2017**, *118*, 247701.
- (13) Bandurin, D. A.; Tyurnina, A. V.; Geliang, L. Y.; Mishchenko, A.; Zólyomi, V.; Morozov, S. V.; Kumar, R. K.; Gorbachev, R. V.; Kudrynskyi, Z. R.; Pezzini, S.; Kovalyuk, Z. D.; Zeitler, U.; Novoselov, K. S.; Patanè, A.; Eaves, L.; Grigoreva, I. V.; Falko, V. I.; Geim, A. K.; Cao, Y. High electron mobility, quantum Hall effect and anomalous optical response in atomically thin InSe. *Nature Nanotechnology* **2017**, *12*, 223–227.
- (14) Wu, Z.; Xu, S.; Lu, H.; Khamoshi, A.; Liu, G.-B.; Han, T.; Wu, Y.; Lin, J.; Long, G.; He, Y.; He, Y.; Cai, Y.; Yao, Y.; Zhang, F.; Wang, N. Even–odd layer-dependent magnetotransport of high-mobility Q-valley electrons in transition metal disulfides. *Nature Communications* **2016**, *7*, 12955.
- (15) Raja, A.; Chaves, A.; Yu, J.; Arefe, G.; Hill, H. M.; Rigosi, A. F.; Berkelbach, T. C.; Nagler, P.; Schüller, C.; Korn, T.; Nuckolls, C.; Hone, J.; Brus, L. E.; Heinz, T. F.; Reichman, D. R.; Chernikov, A. Coulomb engineering of the bandgap and excitons in two-dimensional materials. *Nature Communications* **2017**, *8*, 15251.
- (16) Xiao, D.; Liu, G.-B.; Feng, W.; Xu, X.; Yao, W. Coupled spin and valley physics in

- monolayers of MoS₂ and other group-VI dichalcogenides. *Physical Review Letters* **2012**, *108*, 196802.
- (17) Xu, X.; Yao, W.; Xiao, D.; Heinz, T. F. Spin and pseudospins in layered transition metal dichalcogenides. *Nature Physics* **2014**, *10*, 343–350.
- (18) Wang, Q. H.; Kalantar-Zadeh, K.; Kis, A.; Coleman, J. N.; Strano, M. S. Electronics and optoelectronics of two-dimensional transition metal dichalcogenides. *Nature Nanotechnology* **2012**, *7*, 699–712.
- (19) Mak, K. F.; He, K.; Shan, J.; Heinz, T. F. Control of valley polarization in monolayer MoS₂ by optical helicity. *Nature Nanotechnology* **2012**, *7*, 494–498.
- (20) Zeng, H.; Dai, J.; Yao, W.; Xiao, D.; Cui, X. Valley polarization in MoS₂ monolayers by optical pumping. *Nature Nanotechnology* **2012**, *7*, 490–493.
- (21) Lagarde, D.; Bouet, L.; Marie, X.; Zhu, C. R.; Liu, B. L.; Amand, T.; Tan, P. H.; Urbaszek, B. Carrier and polarization dynamics in monolayer MoS₂. *Physical Review Letters* **2014**, *112*, 047401.
- (22) Wang, G.; Bouet, L.; Lagarde, D.; Vidal, M.; Balocchi, A.; Amand, T.; Marie, X.; Urbaszek, B. Valley dynamics probed through charged and neutral exciton emission in monolayer WSe₂. *Physical Review B* **2014**, *90*, 075413.
- (23) Robert, C.; Lagarde, D.; Cadiz, F.; Wang, G.; Lassagne, B.; Amand, T.; Balocchi, A.; Renucci, P.; Tongay, S.; Urbaszek, B.; Marie, X. Exciton radiative lifetime in transition metal dichalcogenide monolayers. *Physical Review B* **2016**, *93*, 205423.
- (24) Wang, G.; Palleau, E.; Amand, T.; Tongay, S.; Marie, X.; Urbaszek, B. Polarization and time-resolved photoluminescence spectroscopy of excitons in MoSe₂ monolayers. *Applied Physics Letters* **2015**, *106*, 112101.

- (25) Zhu, C. R.; Zhang, K.; Glazov, M.; Urbaszek, B.; Amand, T.; Ji, Z. W.; Liu, B. L.; Marie, X. Exciton valley dynamics probed by Kerr rotation in WSe₂ monolayers. *Physical Review B* **2014**, *90*, 161302.
- (26) Kang, J.; Tongay, S.; Zhou, J.; Li, J.; Wu, J. Band offsets and heterostructures of two-dimensional semiconductors. *Applied Physics Letters* **2013**, *102*, 012111.
- (27) Rivera, P.; Schaibley, J. R.; Jones, A. M.; Ross, J. S.; Wu, S.; Aivazian, G.; Klement, P.; Seyler, K.; Clark, G.; Ghimire, N. J.; Yan, J.; Mandrus, D. G.; Yao, W.; Xu, X. Observation of long-lived interlayer excitons in monolayer MoSe₂-WSe₂ heterostructures. *Nature Communications* **2015**, *6*, 6242.
- (28) Rivera, P.; Seyler, K. L.; Yu, H.; Schaibley, J. R.; Yan, J.; Mandrus, D. G.; Yao, W.; Xu, X. Valley-polarized exciton dynamics in a 2D semiconductor heterostructure. *Science* **2016**, *351*, 688–691.
- (29) Nagler, P.; Plechinger, G.; Ballottin, M. V.; Mitioglu, A.; Meier, S.; Paradiso, N.; Strunk, C.; Chernikov, A.; Christianen, P. C.; Schüller, C.; Korn, T. Interlayer exciton dynamics in a dichalcogenide monolayer heterostructure. *2D Materials* **2017**, *4*, 025112.
- (30) Miller, B.; Steinhoff, A.; Pano, B.; Klein, J.; Jahnke, F.; Holleitner, A.; Wurstbauer, U. Long-lived direct and indirect interlayer excitons in van der Waals heterostructures. *Nano Letters* **2017**, *17*, 5229–5237.
- (31) Baranowski, M.; Surrente, A.; Klotowski, L.; Urban, J.; Zhang, N.; Maude, D. K.; Wiwatowski, K.; Mackowski, S.; Kung, Y.-C.; Dumcenco, D.; Kis, A.; Plochocka, P. Probing the Interlayer Exciton Physics in a MoS₂/MoSe₂/MoS₂ van der Waals Heterostructure. *Nano Letters* **2017**, *17*, 6360–6365.
- (32) Surrente, A.; Klotowski, L.; Zhang, N.; Baranowski, M.; Mitioglu, A.; Ballottin, M. V.; Christianen, P. C.; Dumcenco, D.; Kung, Y.-C.; Maude, D. K.; Kis, A.;

- Plochocka, P. Intervalley Scattering of Interlayer Excitons in a MoS₂/MoSe₂/MoS₂ Heterostructure in High Magnetic Field. *Nano Letters* **2018**, *18*, 3994–4000.
- (33) Hanbicki, A. T.; Chuang, H.-J.; Rosenberger, M. R.; Hellberg, C. S.; Sivaram, S. V.; McCreary, K. M.; Mazin, I. I.; Jonker, B. T. Double Indirect Interlayer Exciton in a MoSe₂/WSe₂ van der Waals Heterostructure. *ACS Nano* **2018**, *12*, 4719–4726.
- (34) Hsu, W.-T.; Lu, L.-S.; Wu, P.-H.; Lee, M.-H.; Chen, P.-J.; Wu, P.-Y.; Chou, Y.-C.; Jeng, H.-T.; Li, L.-J.; Chu, M.-W.; Chang, W.-H. Negative circular polarization emissions from WSe₂/MoSe₂ commensurate heterobilayers. *Nature Communications* **2018**, *9*, 1356.
- (35) Park, C.-H.; Yang, L.; Son, Y.-W.; Cohen, M. L.; Louie, S. G. Anisotropic behaviours of massless Dirac fermions in graphene under periodic potentials. *Nature Physics* **2008**, *4*, 213–217.
- (36) Xue, J.; Sanchez-Yamagishi, J.; Bulmash, D.; Jacquod, P.; Deshpande, A.; Watanabe, K.; Taniguchi, T.; Jarillo-Herrero, P.; LeRoy, B. J. Scanning tunnelling microscopy and spectroscopy of ultra-flat graphene on hexagonal boron nitride. *Nature Materials* **2011**, *10*, 282–285.
- (37) Yankowitz, M.; Xue, J.; Cormode, D.; Sanchez-Yamagishi, J. D.; Watanabe, K.; Taniguchi, T.; Jarillo-Herrero, P.; Jacquod, P.; LeRoy, B. J. Emergence of superlattice Dirac points in graphene on hexagonal boron nitride. *Nature Physics* **2012**, *8*, 382–386.
- (38) Ponomarenko, L.; Gorbachev, R.; Yu, G.; Elias, D.; Jalil, R.; Patel, A.; Mishchenko, A.; Mayorov, A.; Woods, C.; Wallbank, J.; Mucha-Kruszynski, M.; Piot, B. A.; Potemski, M.; Grigorieva, I. V.; Novoselov, K. S.; Guinea, F.; Falko, V. I.; K, G. A. Cloning of Dirac fermions in graphene superlattices. *Nature* **2013**, *497*, 594–597.

- (39) Yu, H.; Liu, G.-B.; Tang, J.; Xu, X.; Yao, W. Moiré excitons: From programmable quantum emitter arrays to spin-orbit-coupled artificial lattices. *Science Advances* **2017**, *3*, e1701696.
- (40) Zhang, C.; Chuu, C.-P.; Ren, X.; Li, M.-Y.; Li, L.-J.; Jin, C.; Chou, M.-Y.; Shih, C.-K. Interlayer couplings, Moiré patterns, and 2D electronic superlattices in MoS₂/WSe₂ hetero-bilayers. *Science Advances* **2017**, *3*, e1601459.
- (41) Hunt, B.; Sanchez-Yamagishi, J.; Young, A.; Yankowitz, M.; LeRoy, B. J.; Watanabe, K.; Taniguchi, T.; Moon, P.; Koshino, M.; Jarillo-Herrero, P.; Ashoori, R. C. Massive Dirac fermions and Hofstadter butterfly in a van der Waals heterostructure. *Science* **2013**, *340*, 1427–1430.
- (42) Wang, E.; Lu, X.; Ding, S.; Yao, W.; Yan, M.; Wan, G.; Deng, K.; Wang, S.; Chen, G.; Ma, L.; Jung, J.; Fedorov, A. V.; Zhang, Y.; Zhang, G.; Zhou, S. Gaps induced by inversion symmetry breaking and second-generation Dirac cones in graphene/hexagonal boron nitride. *Nature Physics* **2016**, *12*, 1111–1115.
- (43) Dean, C.; Wang, L.; Maher, P.; Forsythe, C.; Ghahari, F.; Gao, Y.; Katoch, J.; Ishigami, M.; Moon, P.; Koshino, M.; Taniguchi, T.; Watanabe, K.; Shepard, K. L.; Hone, J.; Kim, P. Hofstadter's butterfly and the fractal quantum Hall effect in moiré superlattices. *Nature* **2013**, *497*, 598–602.
- (44) Wu, F.; Lovorn, T.; MacDonald, A. Theory of optical absorption by interlayer excitons in transition metal dichalcogenide heterobilayers. *Physical Review B* **2018**, *97*, 035306.
- (45) Wu, F.; Lovorn, T.; Macdonald, A. H. Topological Exciton Bands in Moiré Heterojunctions. *Physical Review Letters* **2017**, *118*, 147401.
- (46) Pan, Y.; Fölsch, S.; Nie, Y.; Waters, D.; Lin, Y.-C.; Jariwala, B.; Zhang, K.; Cho, K.; Robinson, J. A.; Feenstra, R. M. Quantum-Confined Electronic States arising from Moiré Pattern of MoS₂-WSe₂ Heterobilayers. *Nano Letters* **2018**, *18*, 1849–1855.

- (47) Ciarrocchi, A.; Unuchek, D.; Avsar, A.; Watanabe, K.; Taniguchi, T.; Kis, A. Control of interlayer excitons in two-dimensional van der Waals heterostructures. *arXiv preprint arXiv:1803.06405* **2018**,
- (48) Surrente, A.; Dumcenco, D.; Yang, Z.; Kuc, A.; Jing, Y.; Heine, T.; Kung, Y.-C.; Maude, D. K.; Kis, A.; Plochocka, P. Defect Healing and Charge Transfer-Mediated Valley Polarization in MoS₂/MoSe₂/MoS₂ Trilayer van der Waals Heterostructures. *Nano Letters* **2017**, *17*, 4130–4136.
- (49) Ceballos, F.; Bellus, M. Z.; Chiu, H.-Y.; Zhao, H. Ultrafast charge separation and indirect exciton formation in a MoS₂–MoSe₂ van der Waals heterostructure. *ACS Nano* **2014**, *8*, 12717–12724.
- (50) Chen, H.; Wen, X.; Zhang, J.; Wu, T.; Gong, Y.; Zhang, X.; Yuan, J.; Yi, C.; Lou, J.; Ajayan, P. M.; Zhuang, W.; Zhang, G.; Zheng, J. Ultrafast formation of interlayer hot excitons in atomically thin MoS₂/WS₂ heterostructures. *Nature Communications* **2016**, *7*, 12512.
- (51) Wang, K.; Huang, B.; Tian, M.; Ceballos, F.; Lin, M.-W.; Mahjouri-Samani, M.; Boulesbaa, A.; Puretzky, A. A.; Rouleau, C. M.; Yoon, M.; Zhao, H.; Xiao, K.; Duscher, G.; Geohegan, D. B. Interlayer coupling in twisted WSe₂/WS₂ bilayer heterostructures revealed by optical spectroscopy. *ACS Nano* **2016**, *10*, 6612–6622.
- (52) Laturia, A.; Van de Put, M. L.; Vandenberghe, W. G. Dielectric properties of hexagonal boron nitride and transition metal dichalcogenides: from monolayer to bulk. *npj 2D Materials and Applications* **2018**, *2*, 6.
- (53) Conley, H. J.; Wang, B.; Ziegler, J. I.; Haglund Jr, R. F.; Pantelides, S. T.; Bolotin, K. I. Bandgap engineering of strained monolayer and bilayer MoS₂. *Nano letters* **2013**, *13*, 3626–3630.

- (54) Lloyd, D.; Liu, X.; Christopher, J. W.; Cantley, L.; Wadehra, A.; Kim, B. L.; Goldberg, B. B.; Swan, A. K.; Bunch, J. S. Band gap engineering with ultralarge biaxial strains in suspended monolayer MoS₂. *Nano Letters* **2016**, *16*, 5836–5841.
- (55) Castellanos-Gomez, A.; Roldán, R.; Cappelluti, E.; Buscema, M.; Guinea, F.; van der Zant, H. S.; Steele, G. A. Local strain engineering in atomically thin MoS₂. *Nano letters* **2013**, *13*, 5361–5366.
- (56) Zhang, X.-X.; You, Y.; Zhao, S. Y. F.; Heinz, T. F. Experimental evidence for dark excitons in monolayer WSe₂. *Physical Review Letters* **2015**, *115*, 257403.
- (57) Tran, K.; Moody, G.; Wu, F.; Lu, X.; Choi, J.; Singh, A.; Embley, J.; Zepeda, A.; Campbell, M.; Kim, K.; Rai, A.; Autry, T.; Sanchez, D. A.; Taniguchi, T.; Watanabe, K.; Lu, N.; Banerjee, S. K.; Tutuc, E.; Yang, L.; MacDonal, A. H.; Silverman, K. L.; Li, X. Moiré Excitons in Van der Waals Heterostructures. *arXiv preprint arXiv:1807.03771* **2018**,
- (58) Wang, G.; Palleau, E.; Amand, T.; Tongay, S.; Marie, X.; Urbaszek, B. Polarization and time-resolved photoluminescence spectroscopy of excitons in MoSe₂ monolayers. *Applied Physics Letters* **2015**, *106*, 112101.
- (59) Kioseoglou, G.; Hanbicki, A. T.; Currie, M.; Friedman, A. L.; Jonker, B. T. Optical polarization and intervalley scattering in single layers of MoS₂ and MoSe₂. *Scientific Reports* **2016**, *6*, 25041.
- (60) Baranowski, M.; Surrente, A.; Maude, D.; Ballottin, M.; Mitioglu, A.; Christianen, P.; Kung, Y.; Dumcenco, D.; Kis, A.; Plochocka, P. Dark excitons and the elusive valley polarization in transition metal dichalcogenides. *2D Materials* **2017**, *4*, 025016.
- (61) Stier, A. V.; Wilson, N. P.; Clark, G.; Xu, X.; Crooker, S. A. Probing the influence of dielectric environment on excitons in monolayer WSe₂: insight from high magnetic fields. *Nano Letters* **2016**, *16*, 7054–7060.

- (62) Kunstmann, J.; Mooshammer, F.; Nagler, P.; Chaves, A.; Stein, F.; Paradiso, N.; Plechinger, G.; Strunk, C.; Schüller, C.; Seifert, G.; Reichman, D. R.; Korn, T. Momentum-space indirect interlayer excitons in transition metal dichalcogenide van der Waals heterostructures. *Nature Physics* **2018**, *14*, 801–805.
- (63) Castellanos-Gomez, A.; Buscema, M.; Molenaar, R.; Singh, V.; Janssen, L.; Van Der Zant, H. S.; Steele, G. A. Deterministic transfer of two-dimensional materials by all-dry viscoelastic stamping. *2D Materials* **2014**, *1*, 011002.
- (64) Frisenda, R.; Navarro-Moratalla, E.; Gant, P.; De Lara, D. P.; Jarillo-Herrero, P.; Gorbachev, R. V.; Castellanos-Gomez, A. Recent progress in the assembly of nanodevices and van der Waals heterostructures by deterministic placement of 2D materials. *Chemical Society Reviews* **2018**, *47*, 53–68.
- (65) Frisenda, R.; Niu, Y.; Gant, P.; Molina-Mendoza, A. J.; Schmidt, R.; Bratschitsch, R.; Liu, J.; Fu, L.; Dumcenco, D.; Kis, A.; Perez De Lara, D.; Castellanos-Gomez, A. Micro-reflectance and transmittance spectroscopy: a versatile and powerful tool to characterize 2D materials. *Journal of Physics D: Applied Physics* **2017**, *50*, 074002.

Graphical TOC Entry

